JLB

Article

Hypomorphic mutation in the RAG2 gene affects dendritic cell distribution and migration

Virginia Maina,[*,†] Veronica Marrella,*[*,†] Stefano Mantero,*[*,†] Barbara Cassani,*[*,†] Elena Fontana,[‡] Achille Anselmo,[†] Annalisa Del Prete,[†,‡] Silvano Sozzani,[†,‡] Paolo Vezzoni,*[*,†] Pietro Luigi Poliani,[‡] and Anna Villa*[*,†,1]

*Milan Unit, Istituto di Ricerca Genetica e Biomedica, Consiglio Nazionale delle Ricerche, Milan, Italy; †Humanitas Clinical and Research Center, Rozzano, Milan, Italy; and ‡Department of Molecular and Translational Medicine, University of Brescia, Italy

RECEIVED JULY 4, 2013; REVISED AUGUST 20, 2013; ACCEPTED SEPTEMBER 3, 2013. DOI: 10.1189/jlb.0713365

ABSTRACT

OS is a severe combined immunodeficiency characterized by erythrodermia and protracted diarrhea as a result of infiltration of oligoclonal-activated T cells, caused by hypomorphic mutations in RAGs. The *RAG2*^{R229Q} mouse model fully recapitulates the clinical OS phenotype. We evaluated whether T and B cell defects, together with the abnormal lymphoid structure, could affect DC homeostasis and function. High density of LCs was observed in skin biopsies of Omenn patients and in the derma of *RAG2*^{R229Q} mice, correlating with the presence of erythrodermia. In vivo models of cutaneous skin painting and CHS demonstrated a decreased migration of *RAG2*^{R229Q} DCs—in particular, LCs—into draining LNs. Interestingly, at steady state, *RAG2*^{R229Q} mice showed a reduction in DC number in all hematopoietic organs except LNs. Analysis of the MHCII marker revealed a diminished expression also upon the LPS-driven inflammatory condition. Despite the decreased number of peripheral DCs, BM pre-cDCs were present in normal number compared with RAG2$^{+/+}$ controls, whereas pDCs and monocytes were reduced significantly. Overall, these results point to a secondary defect in the DC compartment, which contributes to clinical manifestations and autoimmunity in OS. *J. Leukoc. Biol.* 94: 1221–1230; 2013.

Introduction

OS is a genetically inherited disorder characterized by severe infections, erythrodermia, and protracted diarrhea as a result of cellular infiltration [1]. Hypomorphic mutations in RAG genes causing a defective but not abolished variable-diversity-joining recombination process are the main responsible for OS, although other genes have been described to cause the disease [1, 2]. In this context, oligoclonal T cells with a restricted TCR repertoire are generated and undergo homeostatic proliferation in the periphery as a result of the lymphopenic condition, leading to the development of immunopathology. Patients present hypereosinophilia, very few circulating B cells, hypogamma-globulinemia, but increased serum IgE [3, 4]. We have described previously a RAG mouse mutant carrying a hypomorphic mutation in the RAG2 gene (R229Q), which mimics many of the clinical features of OS. *RAG2*^{R229Q} mice show marked infiltration of T lymphocytes and eosinophils in the skin and gut, which contrasts with the overall lymphoid depletion observed in thymus, LNs, and spleen [5, 6]. Similarly to OS patients, *RAG2*^{R229Q} murine thymi have abnormal architecture, nearly absent mTEC, and barely detectable expression of autoimmune regulatory elements, causing altered negative selection of autoreactive T cells that escape to the periphery and damage target organs. Peripheral lymphoid organ architecture is compromised severely [6, 7]. A dramatic decrease in Forkhead p3^{+} nTregs is observed in humans and mice, indicating impairment in central and peripheral tolerance [5, 8]. A still poorly explored cell compartment in OS is represented by DCs, whose maturation, migration, survival, and production of cytokines are influenced by T cell-derived signals [9–11]. Moreover, the T cell area contributes to LN architecture, thus influencing DC retention into the LNs [12]. In OS patients, thymic DCs are reduced severely and distributed abnormally [13]. Conversely, DCs are present in OS patients' skin biopsies [14], and the accumulation observed in LNs—so-called "dermatopathic reac-

Abbreviations: ^{3}H=titrated thymidine, 5HPF=five high-power field, BDCA2=blood DC antigen 2, BM=bone marrow, BM-DC=bone marrow-derived DC, cDC=conventional DC, CDP=common DC precursor, CHS=contact hypersensitivity, CLP=common lymphoid precursor, CMP=common myeloid precursor, FFPE=formalin-fixed paraffin-embedded, GMP=granulocyte macrophage precursor, IDC=interdigitating DC, DC-LAMP= dendritic cell-lysosome-associated membrane glycoprotein, LC=Langerhans cell, Lin=lineage, MLR=mixed leukocyte reaction, Mo-DC=monocyte-derived DC, mTEC=medullary thymic epithelial cell, nTreg=naturally occurring regulatory T cell, OS=Omenn syndrome, OXA=oxazolone, 4, ethoxymethylene-2-phenil-2-oxazolin-5-one, pDC=plasmacytoid DC, PDCA1=plasmacytoid DC antigen 1, pre-cDC=conventional DC precursor, Sirp-α=signal regulatory protein-α

The online version of this paper, found at www.jleukbio.org, includes supplemental information.

1. Correspondence: Humanitas Clinical and Research Center, via Manzoni 56, 20089, Rozzano (Milan), Italy. E-mail: anna.villa@humanitasresearch.it

tion"—is considered a typical clinical feature [15]. Here, we have investigated whether hypomorphic RAG defects in lymphocytes could, in turn, perturb DCs homeostasis, thus contributing to the immune dysregulation observed in OS. The analysis of the DC subpopulation in thymus, spleen, and peripheral lymphoid organs of mutant mice shows abnormal subset distribution and alteration in their activation state. Moreover, we demonstrate an impaired DC migration from skin to the LN at steady state and in inflammatory conditions. These findings well correlate with our observation of LC accumulation in the skin of OS patients. Overall, these data suggest a role of *RAG2*^{R229Q} DCs in the pathogenesis of immunodeficiency and autoimmunity in OS.

MATERIALS AND METHODS

Patients

Human formalin-fixed, paraffin-embedded tissue samples were retrieved from the archive of the Department of Pathology at Spedali Civili of Brescia (Italy), in accordance with the protocols of the Spedali Civili of Brescia Institutional Ethical Board. Skin specimens from Patient 1, who was compound heterozygous in RAG1 gene (R396H/I538fr; named OS4 in ref. [16]), and from Patient 2, carrying a mis-sense mutation (R229Q) in the RAG2 gene (described in ref. [17]), were analyzed for the presence of Langerin$^+$ cells in the epidermal and derma layers. Both patients presented typical signs of OS, characterized by generalized erythrodermia associated with lymphoadenopathy, failure to thrive, and eosinophilia.

Mice

129Sv/C57/BL6 Knock-in *RAG2*^{R229Q} and 129Sv/C57/BL6 RAG2$^{+/+}$ mice were generated as described previously [5]. All animals (8–12 weeks old) were housed in a specific pathogen-free facility. All procedures were approved by the Institutional Animal Care and Use Committee (Minister of Health; Protocol No. 9/2011). All possible efforts were taken to avoid animal suffering at any stage of the experiments.

FACS and analysis

Single-cell suspensions were obtained from thymus, spleens, LNs, and BM. Red blood cells were lysed in ACK lysis buffer (Sigma, St. Louis, MO, USA). Unless otherwise indicated, 10^6 cells were stained in FACS buffer with the following mAb purchased by BD PharMingen (San Diego, CA, USA), or eBioscience (San Diego, CA, USA): CD45 (30-F11, BD Pharmingen), CD16/32 (93, eBioscience), CD11c (N418, eBioscience), CD8a (53-6.7, eBioscience), B220 (RA3-6B2, BD Pharmingen), CD11b (M1/70, eBioscience and BD Pharmingen), Sirp-α (CD172a, P84, BD Pharmingen), PDCA1 (CD317, eBio129C, eBioscience), Siglec H (eBio440C, eBioscience), Langerin (CD207, EBioL31, eBioscience) [18], CD115 (AFS98, eBioscience), Ly6C (AL-21, BD Pharmingen), Ly6G (1A8, BD Pharmingen), MHCII (IAb, M5/114.15.2, eBioscience), CD80 (16-10A1, BD Pharmingen), CD86 (B7-2, BD Pharmingen), CD40 (3/23, BD Pharmingen), mouse hematopoietic Lin cocktail (eBioscience), *Sca*I (D7, eBioscience), c-Kit (CD117, 2B8, eBioscience), IL-7Rα (CD127, A7R34, eBioscience), CD34 (RAM34, eBioscience), CD135 (A2F10, eBioscience), CD45RA (14.08, BD Pharmingen), CD49b (DX5, eBioscience), and CD19 (1D3, eBioscience). After analyzing pDCs (CD11c$^+$, B220$^+$, Siglec H$^+$, PDCA1$^+$), cDCs were divided in CD8$^+$cDCs (CD11c$^+$ CD8a$^+$ CD11b$^-$) and CD8$^-$cDCs (CD11c$^+$ CD8$^-$ CD11b$^+$). In the thymus, cDCs were also identified as CD8$^-$Sirp-α$^+$ or CD8$^+$Sirp-α$^-$. Mo-DCs [19, 20] were identified as CD11c$^+$CD11b$^+$CD8$^-$Ly6C$^+$ cells after excluding pDCs and neutrophils (CD11b$^+$Ly6G$^+$). Where indicated, in LNs, we distinguished: CD11b^{hi} Langerin$^-$, CD8$^+$Langerin$^-$, skin-derived CD11b^{lo}Langerin$^+$ and CD11b$^+$ Langerin$^+$, blood-derived LN resident CD8$^+$Langerin$^+$ DCs [21, 22]. In the BM, we identified: CLPs as Lin$^-$*Sca*I^{lo}CD135$^+$IL-7Rα$^+$ckit^{lo}, CMPs as Lin$^-$*Sca*I$^-$IL-7Rα$^-$cKit^{hi}CD16/32^{lo}CD34$^+$, GMPs as Lin$^-$IL-7Rα$^-$*Sca*I$^-$cKit^{hi} CD16/32^{hi}CD34^{hi}, CDPs as Lin$^-$IL-7Rα$^-$cKit^{int}CD135$^+$CD115$^{hi/lo/+}$, pDCs as CD11c^{int}DX5$^-$CD19$^-$CD45RA$^+$, monocytes as CD45$^+$CD11b$^+$ Ly6G$^-$Ly6C$^+$, and precDCs as Lin$^-$CD11c$^+$MHCII$^-$ [23–25]. The fluorescence-minus-one correction method was used for all antibodies tested [26]. Samples were acquired with FACSCanto II System (BD Biosciences), and data were analyzed with DIVA Software (Version 6.1.3; BD Biosciences) and/or FlowJo software (Version 7.6.1; TreeStar, Ashland, OR, USA).

BM-DC generation and in vitro characterization

RAG2$^{+/+}$ and *RAG2*^{R229Q} BM cells were flushed, and CD34$^+$ precursors were cultured for 8 days in RPMI 1640 (Lonza, Walkersville, MD, USA) containing 1% penicillin-streptomycin (Lonza), 5% FBS (Lonza), and 5×10^{-5} M 2β-ME (Sigma), and conventional BM-DCs were differentiated with 100 ng/ml human Fms-like tyrosine kinase 3 ligand and 40 ng/ml murine GM-CSF (PeproTech, Rocky Hill, NJ, USA). RAG2$^{+/+}$ and RAG2^{R229Q} conventional BM-DCs were matured with LPS 100 ng/ml for 24 h. IL-12-p70 production by immature and LPS-matured *RAG2*^{R229Q} and RAG2$^{+/+}$ BM-DCs was evaluated by ELISA (R&D Systems, Minneapolis, MN, USA). For MLR experiments, splenic BALB/c (Charles River Laboratories, Wilmington, MA, USA) CD90$^+$ cells were purified by CD90.2 microbeads (Miltenyi Biotec, Auburn, CA, USA), and 3×10^5 T cells were resuspended in 100 μl MLR medium (RPMI 1640, 10% FBS, 50 mM, 2β-ME) and cocultured with 3×10^4 RAG2$^{+/+}$ and *RAG2*^{R229Q} immature and LPS-matured BM-DCs, making 1:3 dilutions in triplicates. After 72 h, 1 μCi ^{3}H (Amersham, Piscataway, NJ, USA) was added for 24 h, and ^{3}H incorporation was evaluated by a liquid scintillator β-counter (Wallac Oy 1450 MicroBeta). For in vitro chemotaxis assay, immature and mature RAG2$^{+/+}$ and *RAG2*^{R229Q} BM-DCs migration toward selected chemokines was evaluated using a chemotaxis chamber (Neuroprobe, Pleasanton, CA, USA) and polycarbonate filter (5 μm pore size; Neuroprobe). Cell suspension (50 μl; 1.5×10^6 cells/ml) was incubated at 37°C for 90 min. The stimuli (30 μl; 100 ng/mL) were added in the lower chamber, and 50 μl DCs (1.5×10^6/ml) were plated in each well. Results were expressed as the mean number of migrated cells in 5HPF.

In vivo migration of murine DCs

LPS-matured *RAG2*$^{+/+}$ and RAG2^{R229Q} BM-DCs were incubated with 1 μM of the vital dye CFSE (Molecular Probes, Eugene, OR, USA) for 15 min at 37°C. CFSE-labeled BM-DCs (10^6 cells) were injected in the left footpad of each treated mouse, and the contralateral footpad was injected with PBS. After 24 h, popliteal LN draining each footpad was recovered, mechanically disaggregated, enzymatically digested with a mixture of collagenase D (1 mg/ml; Roche, Mannheim, Germany) and DNAse I (0.4 mg/ml; Roche), and incubated for 30 min at 37°C. The single-cell suspension obtained was counted, and CD11c$^+$/CFSE$^+$ cells were analyzed by FACS. Dedicated popliteal draining LNs were mechanically destroyed in 250 μl PBS without Ca^{++} and Mg^{++} using TissueLyser (Qiagen, Valencia, CA, USA). The resulting homogenate was centrifuged, and the supernatants were assessed by dedicated ELISA assays for TNF-α, CCL2, CCL17, and CCL21 (R&D Systems).

FITC skin-painting model

Mice were painted on shaved abdomen with 0.2 ml (5 mg/ml) FITC isomer I (Sigma), dissolved previously 50:50 (vol:vol) in acetone:dibutylphtalate. After 24 and 48 h, inguinal LNs were disaggregated and enzymatically digested, and CD11c$^+$/FITC$^+$ cells were evaluated by FACS.

CHS reaction

CHS was induced by the hapten OXA (Sigma), freshly prepared at 3% in the vehicle (acetone:olive oil, 4:1) and painted at Day −5 on the shaved abdomen for sensitization as follows: 50 μl on inguinal LNs, 50 μl auxillary and brachial LNs, and 5 μl for on each footpad (20 μl/mouse). On Day 0, mice were challenged by painting the left ear with 1% OXA (20 μl) and the right ear with the vehicle alone. Ear swelling was measured starting from 24 to 72 h after

painting [27]. At the sacrifice, ears and draining LNs were collected for immunohistochemistry. For FACS analysis, ear-draining LNs were enzymatically digested, and 5×10^6 cells were stained for LC identification [28].

In vivo LPS stimulation

LPS was injected i.p. (100 ng/g body weight), and mice were killed 6 h after treatment [29]. To analyze splenic DC exhaustion, LPS (1 μg/g body weight) was injected i.p., and mice were killed after 24, 48, and 72 h [30].

Immunohistochemistry

For single and double immunostains, both fresh-frozen and FFPE tissues have been used. Five μm thick cryostat sections were air-dried and fixed in acetone, whereas 2 μm-thick FFPE sections were dewaxed and rehydrated and endogenous peroxidase activity blocked by 0.3% H_2O_2/methanol for 20 min. Heat-induced antigen retrieval was obtained by microwave treatment or incubation in a thermostatic bath using EDTA buffer, pH 8.0. As primary antibodies, we used: biotinylated anti-mouse CD11c (BD PharMingen; 1:100), anti-human CD11c (Monosan, Uden, Netherlands; 1:50), anti-mouse Langerin (Dendritics, Lyon, France; 1:200), anti-human Langerin (Vector Laboratories, Burlingame, CA, USA; 1:150), anti-CD3 (Thermo Scientific, Waltham, MA, USA; 1:100), anti-human CD1a (Dako Cytomation, Denmark; 1: 50), anti-CD40 (Leica Biosystems, Wetzlar, Germany; 1: 60), anti-DC-LAMP (Instrumentation Laboratory, Werfen Life Group, Bedford, MA, USA; 1:100), anti-S100 (Dako Cytomation; 1:3000), and anti-BDCA2 (Dendritics; 1:75). Depending on the primary antibodies used, sections were then incubated with different kits: 4plus Streptavidin HRP Label (Biocare Medical, Concord, CA, USA); Rat-on-Mouse HRP-Polymer (Biocare Medical); real EnVision rabbit/mouse HRP-labeled polymer system (Dako Cytomation); and MACH 4 AP-Polymer (Biocare Medical). Reactions were developed in Biocare's Betazoid DAB and Ferangi Blue (alkaline phosphatase substrate; Biocare Medical) and counterstained with hematoxylin or Methyl Green (Bio-Optica, Milan, Italy). Digital images were acquired by an Olympus DP70 camera mounted on an Olympus Bx60 microscope, using Cell^F Imaging software (Olympus Soft Imaging System GmbH, Germany). Langerin$^+$ cells were counted on different 5HPF (corresponding to 1 mm^2 tissue) for each section, selecting areas with the highest number of positive cells, using the Nikon Eclipse 50i microscope. Values are expressed as number of cells/mm^2.

Statistical analysis

Groups were analyzed with Prism Software (Graph Pad Software, La Jolla, CA, USA) using unpaired, two-tailed Student's *t*-test comparing the experimental group and control. Data were expressed as mean ± SEM. A P value <0.05 was considered significant.

RESULTS

LCs accumulate in the skin of Omenn patients and RAG2^{R229Q} mice

Skin manifestations represent the clinical hallmark of OS, and skin eruptions are present frequently in the OS murine counterpart [5, 6]. LCs have been implicated as aggravators of skin diseases [28, 31] by activating self-antigen-specific T cells and initiating autoimmune responses [32]. Careful analysis of OS patients' skin biopsies has revealed an increased number of Langerin$^+$ cells in the derma compared with healthy donors (**Fig. 1A**). Given the obvious limitations in performing experiments with tissue samples from Omenn patients, we have addressed the involvement of DCs in OS pathogenesis using the *RAG2*^{R229Q} murine model. Interestingly, the majority of Langerin$^+$ cells was localized in the derma of mutant mice, and their density increased considerably in *RAG2*^{R229Q} skin with severe erythrodermia (Fig. 1B).

As DCs are involved in the dermatopathic reaction occurring in OS LNs [15], we further characterized DC subsets in affected LNs specimens. A predominance of S100$^+$ and CD11c$^+$ LN DCs was found and within S100$^+$ cell subsets, IDCs (S100$^+$CD1a$^-$ Langerin$^-$) and LCs (S100$^+$CD1a$^+$Langerin$^+$), and indeterminate cells (S100$^+$CD1a$^+$Langerin$^-$) were observed [15, 33, 34]. Notably, the most represented S100$^+$ DC in OS LN were IDCs and indeterminate cells, considered as immature precursors of LCs [35]. These data suggest that IDCs preferentially accumulate in the LNs, where they might contribute to the dermatopathic reaction described in OS LNs (Fig. 1B), whereas Langerin$^+$ cells remain localized mainly in the derma (Fig. 1A, upper graph).

Normal number of CD11c$^+$ cells in *RAG2*^{R229Q} LNs at steady state and reduced migration in inflammatory conditions

To understand whether the accumulation of Langerin$^+$ cells in OS patients and mouse skin reflects a defect in migration to the LNs, we have evaluated DCs at steady state and in inflammatory conditions. At steady state, *RAG2*^{R229Q} draining LNs, although reduced in size and cellularity compared with controls [5, 6], showed a normal number and increased percentage of CD11c$^+$ DCs evaluated by FACS analysis (**Fig. 2A**, left and right). Immunohistochemistry for CD11c and CD3 showed a similar density of DCs in *RAG2*^{R229Q} compared with RAG2$^{+/+}$ LNs (Fig. 2B). Among DC subsets, only CD8$^+$ cDCs were lower in number in *RAG2*^{R229Q} compared with RAG2$^{+/+}$ LNs (Fig. 2C, left). Moreover, we observed an increased frequency of Mo-DCs [19] (identified as CD11c$^+$CD11b$^+$CD8$^-$B220$^-$PDCA1$^-$ Ly6G$^-$Ly6C$^+$) in *RAG2*^{R229Q} LNs (Fig. 2C, right). Interestingly, MHCII expression was lower in both cDC subsets (Fig. 2D), and a decreased CD80 and CD86 expression was detected in CD8$^-$ cDCs (data not shown). At steady state, LN Langerin$^+$ subsets were reduced numerically compared with controls (Supplemental Fig. 1A). When we evaluated DC distribution in inflammatory conditions induced by FITC skin painting, we found a reduced number of FITC$^+$CD11c$^+$ cells at 24 h in *RAG2*^{R229Q} inguinal LNs, which remained low even at 48 h (**Fig. 3A**). In particular, both skin-derived and LN resident Langerin$^+$ [21, 22] FITC$^+$ subsets were reduced (Supplemental Fig. 1B), including the MHCII$^+$CD11b^{lo}Langerin$^+$ subset (Supplemental Fig. 1C). Next, we induced CHS by FITC (data not shown) or OXA a more powerful hapten [36]. Despite mutant mice showing a reduced ear thickness (Fig. 3B), Langerin$^+$ cells accumulated abnormally in the derma of OXA-stimulated *RAG2*^{R229Q} mice (Fig. 3C, lower right) compared with controls (Fig. 3C, upper right), whereas no differences were noticed in vehicle-treated mice (Fig. 3C, upper and lower left). Importantly, 72 h after CHS, a reduced number of CD11c$^+$ DCs were found in *RAG2*^{R229Q} ear-draining LNs (Fig. 3D), affecting particularly, the different Langerin$^+$ subsets (Fig. 3E). Consistently with OS patients, immunohistochemical analysis did not show an increased recruitment of Langerin$^+$ cells in *RAG2*^{R229Q} ear-draining LNs (data not shown). These data suggest a defective migration of Langerin$^+$ cells from the skin to the LN and a role of LCs in perpetuating skin manifestations in OS patients and mice, as observed in other autoimmune disorders [28, 37].

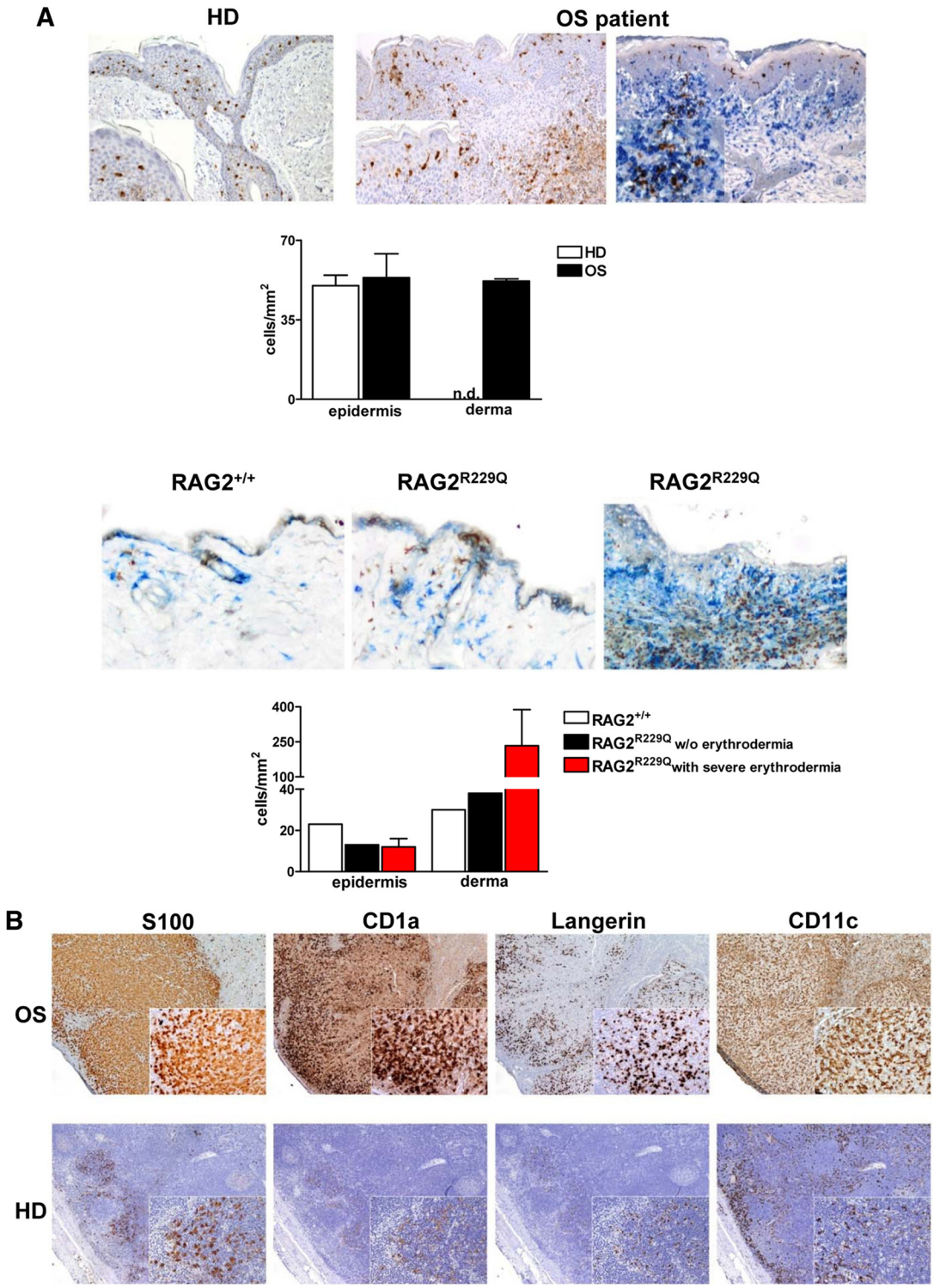

Figure 1. LCs accumulate in skin biopsies from OS patients and mice. (A, upper) Langerin staining (depicted in brown) performed on healthy donor (HD) and OS patient (Patient 1) skin biopsies (upper, middle). (Upper, right) Double staining for Langerin (brown) and CD3 (blue) in OS Patient 2 skin biopsy (original magnification, ×10; inset original magnification, ×20). The upper graph indicates Langerin$^+$ cells/mm^2 performed on epidermal and dermal layers obtained from HDs and OS patients. (Lower) Immunohystochemical analysis of Langerin$^+$ and CD3$^+$ cells performed on the skin of RAG2$^{+/+}$ (left), *RAG2*^{R229Q} mice without skin manifestations (lower, middle panel), and *RAG2*^{R229Q} mice with typical erythrodermia (lower, right; original magnification, ×20). The lower graph shows absolute counts of Langerin$^+$ cells in epidermal and dermal layers in RAG2$^{+/+}$ animals and *RAG2*^{R229Q} mice, with and without erythrodermia. (B) S100, CD1a, Langerin, and CD11c stainings on serial sections of the same LN from an Omenn patient (Patient 2; original magnification, ×10; inset original magnification, ×20) and a normal LN.

Abnormal *RAG2*^{R229Q} LN structure affects DC recruitment in inflammatory conditions

To evaluate the functionality of *RAG2*^{R229Q} DCs, we generated BM-DCs and tested their function in in vitro assays. *RAG2*^{R229Q} BM-DCs did not show defects in the production of IL-12-p70 upon LPS stimulation (Supplemental Fig. 2B). In a MLR assay, the ability of *RAG2*^{R229Q} BM-DCs to induce naïve, allogenic T cell proliferation was comparable with control BM-DCs (Supplemental Fig. 2C). Moreover, in in vitro chemotaxis assays, mutant immature and mature BM-DCs did not show migratory alterations in the presence of CCL3, CCL5, and CCL19, respectively (Supplemental Fig. 2D). Next, we evaluated in vivo migration toward popliteal LNs of CFSE-labeled RAG2$^{+/+}$ and *RAG2*^{R229Q} BM-DCs, s.c.-injected into the footpad of mutant or control mice. Al-

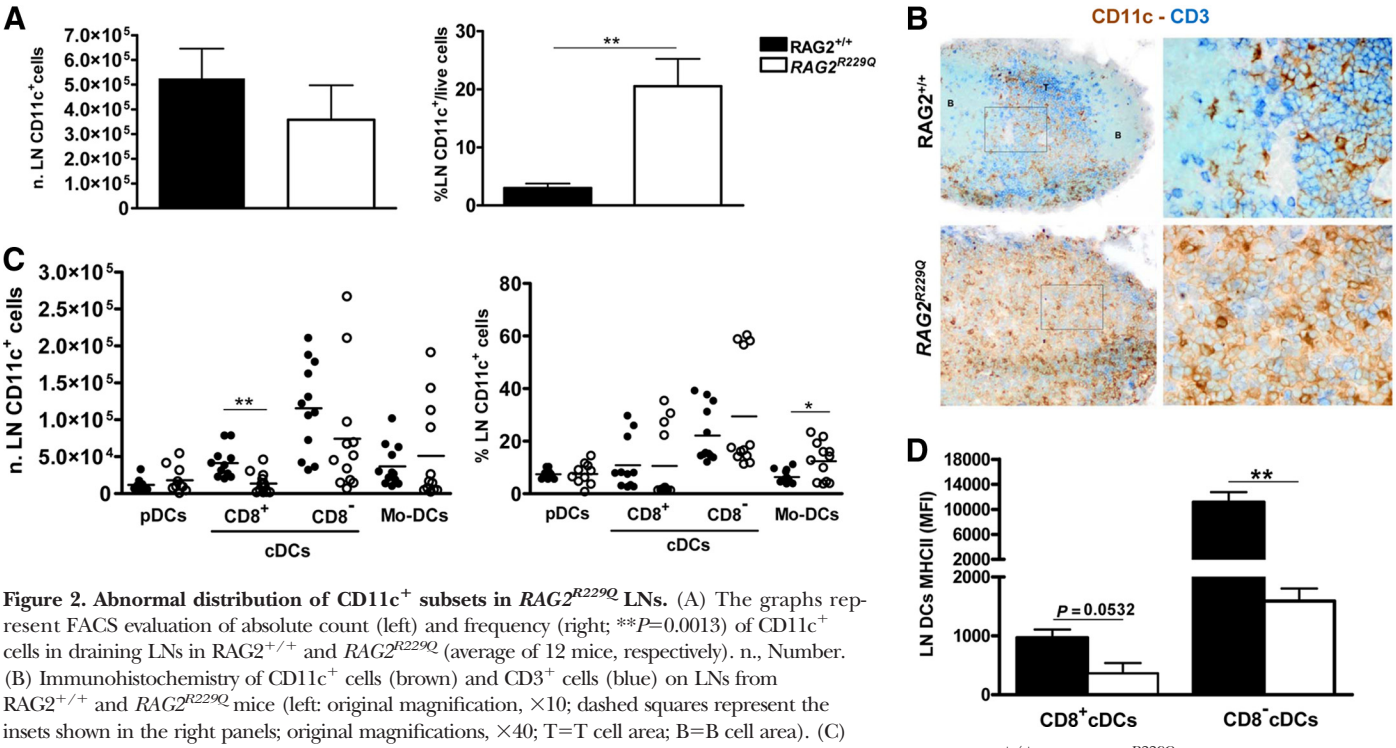

Figure 2. Abnormal distribution of CD11c$^+$ subsets in *RAG2^{R229Q}* LNs. (A) The graphs represent FACS evaluation of absolute count (left) and frequency (right; $^{**}P$=0.0013) of CD11c$^+$ cells in draining LNs in RAG2$^{+/+}$ and *RAG2^{R229Q}* (average of 12 mice, respectively). n., Number. (B) Immunohistochemistry of CD11c$^+$ cells (brown) and CD3$^+$ cells (blue) on LNs from RAG2$^{+/+}$ and *RAG2^{R229Q}* mice (left: original magnification, ×10; dashed squares represent the insets shown in the right panels; original magnifications, ×40; T=T cell area; B=B cell area). (C) Number (left; $^{**}P$=0.001) and frequency distribution (right; $^{*}P$=0.01) of cDCs, pDCs, and Mo-DCs between RAG2$^{+/+}$ and *RAG2^{R229Q}* LN DCs. (D) Mean fluorescence intensity (MFI) of MHCII expression on cDC subsets ($^{**}P$=0.0039).

though the injection of BM-DCs caused an increase in RAG2$^{+/+}$ LN cellularity [38], *RAG2^{R229Q}* LN cell count remained low as in untreated mutants (Supplemental Fig. 2E). Consistent with the atrophic and disorganized OS LN structure [5], the number of RAG2$^{+/+}$ CFSE-labeled BM-DCs isolated from mutant LNs was reduced compared with BM-DCs retrieved in RAG2$^{+/+}$ recipients, in accordance with data observed in other immunodeficient mice [39] (**Fig. 4A**). Our findings indicate that the altered stromal structure of the OS LN has a primary role in determining the abnormal DC recruitment, despite the high levels of TNF-α found in mutant LNs in response to the inflammatory reaction caused by DC injection and the slight increase in chemokines involved in DCs migration [38, 40] (Fig. 4B).

Reduced number and altered distribution of cDCs and pDCs in *RAG2^{R229Q}* thymus

We have described previously that human thymic DCs, identified with CD11c, S100, and BDCA2 immunostainings, were virtually absent in OS patients, and mature, activated, thymic DCs were barely detectable, whereas a significant number of CD11c$^+$ cells coexpressed CD163, representing macrophages [13]. As defect in central tolerance has been reported previously in OS patients and murine counterpart, caused by defective epithelial-thymocyte cross-talk and aberrant thymic architecture [5, 7, 13], and as DCs contribute to the clonal deletion of autoreactive T cells and generation of nTreg cells [41], we have evaluated the DC distribution and activation state in *RAG2^{R229Q}* thymi. As a result of the reduced organ cellularity, *RAG2^{R229Q}* DCs were increased in frequency, although reduced significantly in number among live cells (**Fig. 5A**, left and right). Moreover, DCs were dispersed into the disorganized thymic structure, and an increased presence of F4/80$^+$ thymic macrophages was observed in the *RAG2^{R229Q}* cortex (Fig. 5B), similarly to OS patients [13]. Further analysis of *RAG2^{R229Q}* DC subsets revealed a significant reduction in number and frequency of pDCs and CD8$^+$ cDCs, whereas CD8$^-$ cDCs were normal in number (Fig. 5C) and higher in frequency (Supplemental Fig. 3A), showing an inversion in the proportion of *RAG2^{R229Q}* cDC subsets compared with normal thymus. Recently, it was found that the cell-surface Sirp-α clearly segregates thymic DCs in two subsets with different localization and function when costained with CD8 [41]. In *RAG2^{R229Q}* thymus, CD8$^-$Sirp-α^+ "migratory" DCs were more represented in percentage compared with the same RAG2$^{+/+}$ subset and to "thymic resident" CD8$^+$Sirp-α^- *RAG2^{R229Q}* DCs (Supplemental Fig. 3B). Moreover, *RAG2^{R229Q}* CD8$^-$Sirp-α^+ DCs increased in number compared with CD8$^+$Sirp-α^- (Supplemental Fig. 3C). Remarkably, both *RAG2^{R229Q}* cDCs and pDCs displayed a decreased frequency of MHCII$^+$ cells (Supplemental Fig. 3D) and a reduced expression of this marker at single-cell level (Fig. 5D). Moreover, the frequency of CD86-positive cells was reduced significantly compared with controls (Supplemental Fig. 3D). All of these findings indicate severe alterations in the thymic DC distribution and in the maturation process.

RAG2^{R229Q} splenic DCs are reduced in number and show decreased capacity to up-regulate MHCII expression

Similar to the thymus, the spleens of *RAG2^{R229Q}* mice, reduced in size and cellularity [5, 6], showed an increased percentage but reduced absolute number of CD11c$^+$ cells (**Fig. 6A**, left

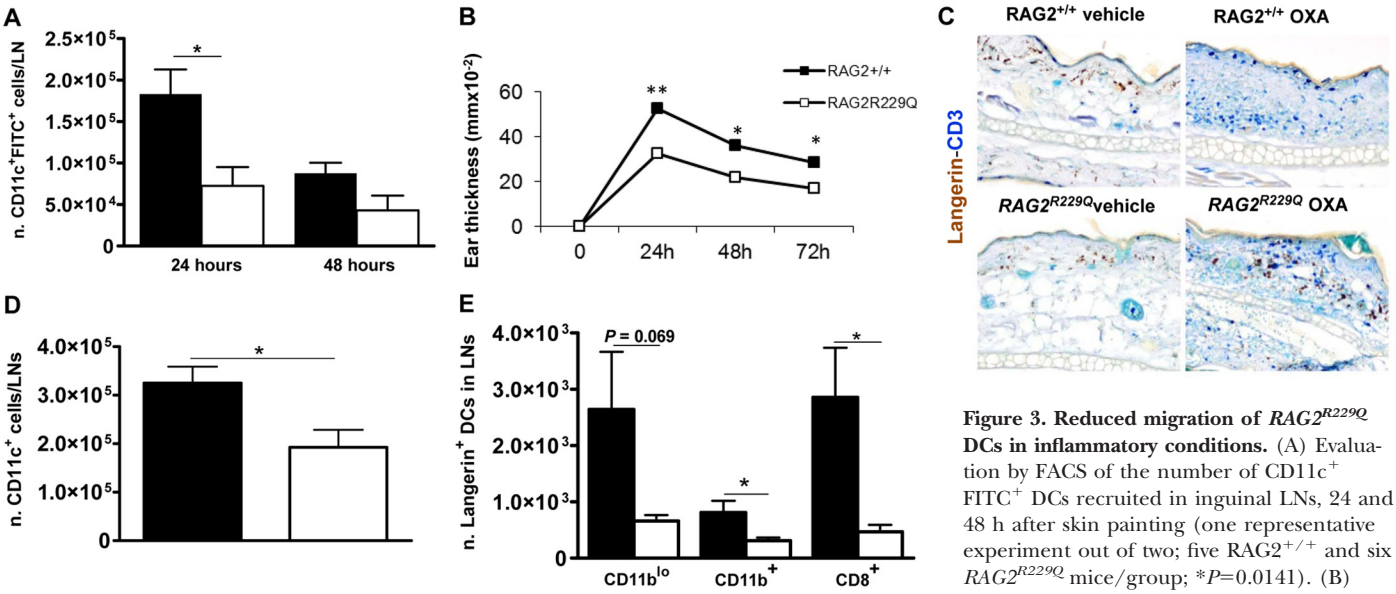

Figure 3. Reduced migration of *RAG2*^{R229Q} DCs in inflammatory conditions. (A) Evaluation by FACS of the number of CD11c$^+$ FITC$^+$ DCs recruited in inguinal LNs, 24 and 48 h after skin painting (one representative experiment out of two; five RAG2$^{+/+}$ and six *RAG2*^{R229Q} mice/group; *P=0.0141). (B) Time course of the response to OXA challenge measured as change in ear thickness (one representative experiment out of two; six mice/group; **P=0.0013; *P=0.034; *P=0.05). (C) Immunostaining for Langerin (brown) and CD3 (blue) on ears from RAG2$^{+/+}$ (upper left) and *RAG2*^{R229Q} (lower left) mice, 72 h after challenge with vehicle (acetone:olive oil, 4:1) or RAG2$^{+/+}$ (upper right) and *RAG2*^{R229Q} (lower right), challenged with OXA. (D) Number of CD11c$^+$ cells recovered in draining LNs, 72 h after CHS induced by OXA (*P=0.0158) and (E) absolute number of Langerin$^+$ subsets in draining LNs, identified as described in Materials and Methods (*P=0.03; *P=0.01).

and right), which were dispersed into the disorganized structure and clustered around a very limited number of CD3$^+$ cells (Fig. 6B). Among CD11c$^+$ cells, CD8$^-$ cDCs and Mo-DCs remained numerically normal (Fig. 6C, left) and increased in frequency (Fig. 6C, right) as the most represented *RAG2*^{R229Q} DC populations. Interestingly, the analysis of the MHCII activation marker showed a lower expression in both cDC subpopulations at steady-state conditions and upon in vivo injection of LPS [29] (Fig. 6D). The reduction in MHCII expression was confirmed further in *RAG2*^{R229Q} BM-DCs induced to differentiate upon LPS stimulation (Supplemental Fig. 2A). Interestingly, in vivo injection of high doses of LPS to induce splenic DC apoptosis [30] showed that the number of *RAG2*^{R229Q} DCs remained nearly constant compared with the reduced number observed in controls (Fig. 6E). All of these data confirm a perturbation in DC distribution and a defective expression of the

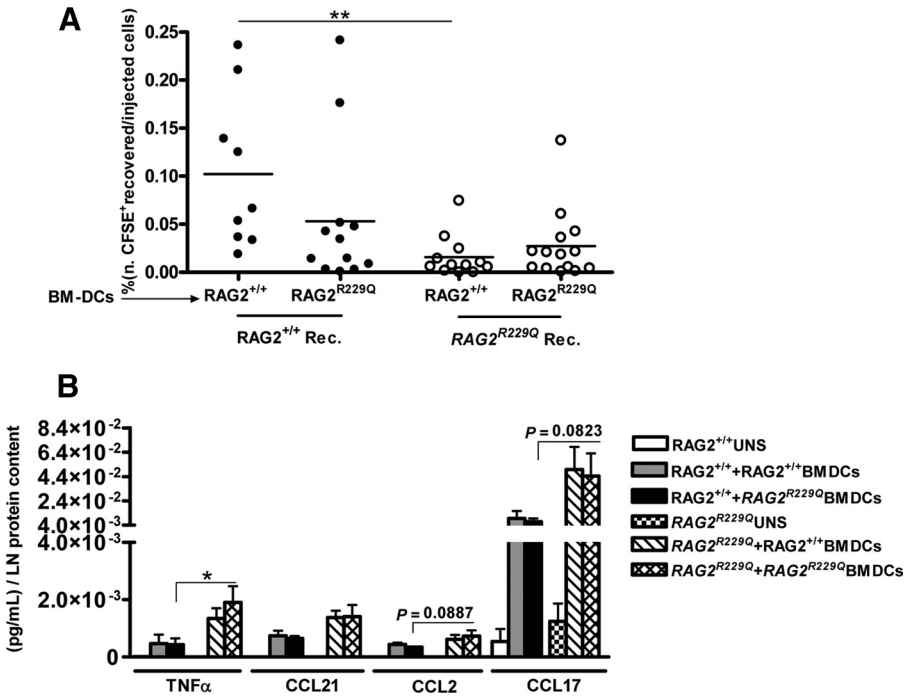

Figure 4. Reduced migration of RAG2$^{+/+}$ CFSE-labeled BM-DCs into *RAG2*^{R229Q} popliteal LN. (A) Evaluation by FACS of the number of CFSE$^+$ BM-DCs recovered in popliteal LN, 24 h after the injection of 10^6 CFSE-labeled BM-DCs in the footpad of RAG2$^{+/+}$ and *RAG2*^{R229Q} recipient (Rec.; average of three experiments performed; **P=0.0019). (B) TNF-α and chemokine quantification by ELISA assays on RAG2$^{+/+}$ and *RAG2*^{R229Q} LN homogenate, 24 h after RAG2$^{+/+}$ and *RAG2*^{R229Q} BM-DC injection (TNF-α; *P=0.045). UNS, unstimulated.

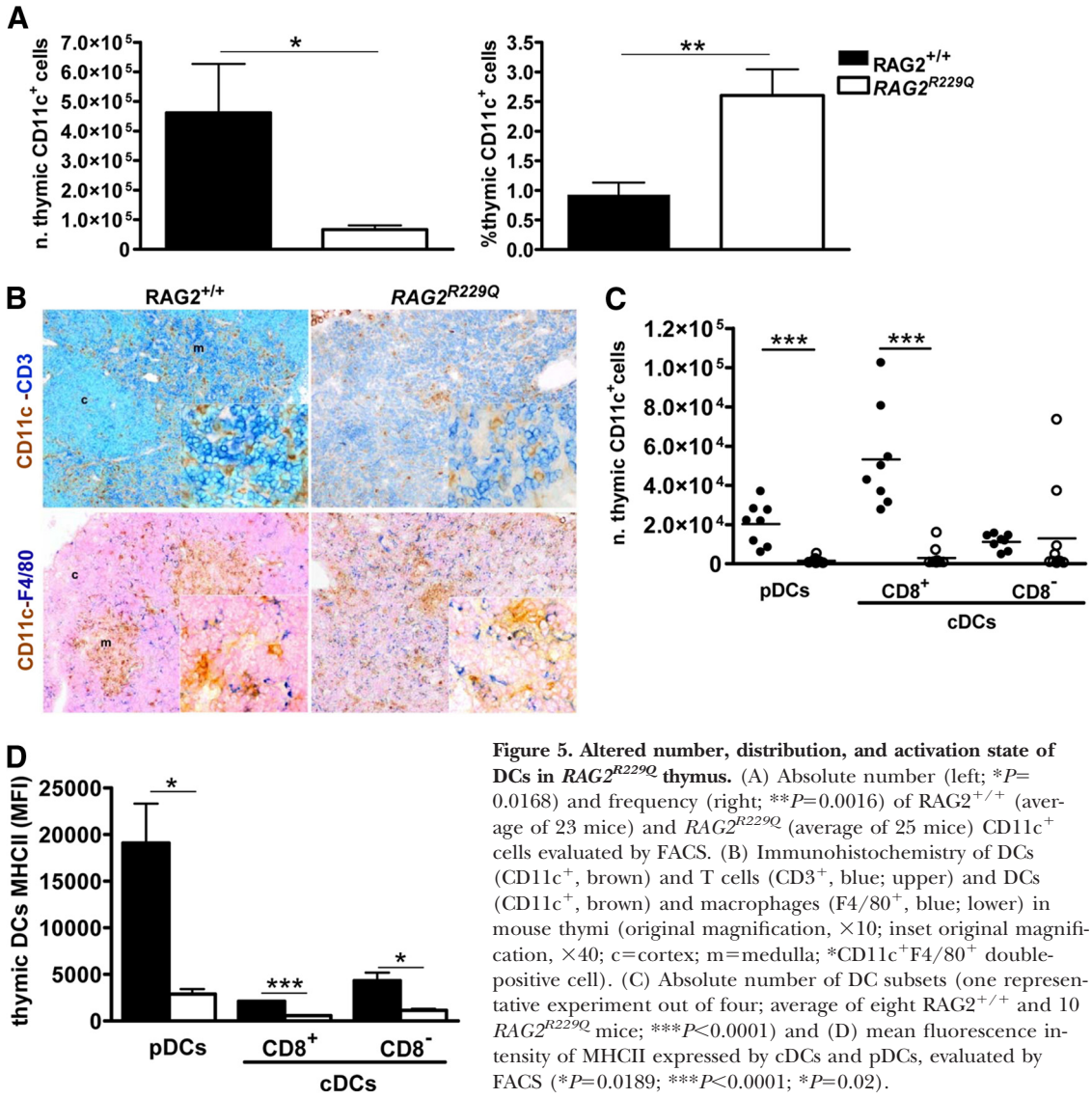

Figure 5. Altered number, distribution, and activation state of DCs in *RAG2*^{R229Q} thymus. (A) Absolute number (left; *P=0.0168) and frequency (right; **P=0.0016) of RAG2$^{+/+}$ (average of 23 mice) and *RAG2*^{R229Q} (average of 25 mice) CD11c^{+} cells evaluated by FACS. (B) Immunohistochemistry of DCs (CD11c^{+}, brown) and T cells (CD3^{+}, blue; upper) and DCs (CD11c^{+}, brown) and macrophages (F4/80^{+}, blue; lower) in mouse thymi (original magnification, ×10; inset original magnification, ×40; c=cortex; m=medulla; *CD11c^{+}F4/80^{+} double-positive cell). (C) Absolute number of DC subsets (one representative experiment out of four; average of eight RAG2$^{+/+}$ and 10 *RAG2*^{R229Q} mice; ***P<0.0001) and (D) mean fluorescence intensity of MHCII expressed by cDCs and pDCs, evaluated by FACS (*P=0.0189; ***P<0.0001; *P=0.02).

activation marker MHCII, also upon LPS induction, which might contribute to the immune dysregulation in OS.

Normal counts of cDC progenitors and a decreased number of pDC precursors and monocytes in *RAG2*^{R229Q} BM

Next, we evaluated whether the reduced number of DCs in lymphoid organs could reflect a defect in the number of their progenitors [23, 24, 42], analyzing *RAG2*^{R229Q} and age-matched control BM samples. Interestingly, BM cellularity was reduced significantly in *RAG2*^{R229Q} compared with RAG2$^{+/+}$ mice (**Fig. 7A**). No differences in the number of CLPs, CMPs, GMPs, and CDPs [24, 25] were present in *RAG2*^{R229Q} BM samples (Fig. 7B). However, the analysis of DC precursors downstream of CDP and GMP revealed a significant decrease in BM pDCs and monocytes, whereas pre-cDCs [24] were not reduced significantly (Fig. 7C). Interestingly, BM-derived pDCs expressed a lower level of MHCII, even at steady-state condition (Supplemental Fig. 4A).

DISCUSSION

The peculiar immunophenotype of leaky SCID associated with autoimmunity, such as OS, represents a unique model to evaluate the effect of activated T cells on DC distribution and function. To this end, using the *RAG2*^{R229Q} mouse model of OS, we have analyzed the effect of the hypomorphic R229Q RAG mutation in lymphocytes on the distribution and function of DCs. We noted in skin biopsies from OS patients an abundance of LCs, which ectopically accumulated in the dermis. Consistently, the murine skin showed high density of LCs at steady state, which increased in inflammatory conditions, correlating with the severity of skin disease. As LCs are involved in maintaining peripheral tolerance [43], their ectopic position in the derma could contribute to the loss of self-tolerance and to the initiation of skin manifestations. Interestingly, few Langerin^{+} cells were found in LNs of OS patients compared with other subsets involved in the dermatopathic reaction. In parallel, *RAG2*^{R229Q} mouse LNs, although reduced in size and disorganized [5], showed a normal number of all DC

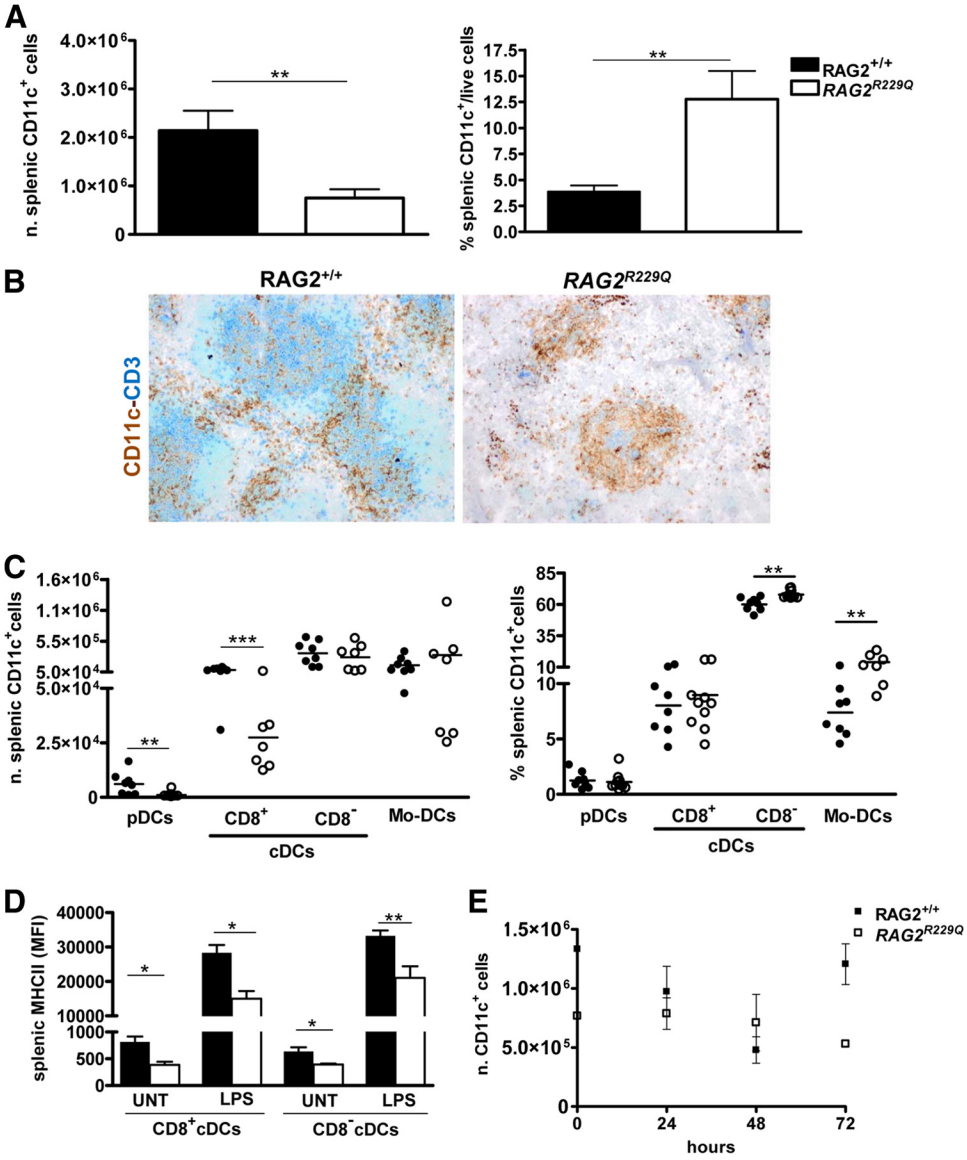

Figure 6. Reduced absolute counts, altered subset distribution, decreased MHCII expression, and altered localization of DCs in *RAG2*^{R229Q} spleen. (A) The graphs show absolute counts (left; $^{**}P$=0.0029) and frequency (right; $^{**}P$=0.003) of splenic RAG2$^{+/+}$ (average of 23 mice) and *RAG2*^{R229Q} (average of 25 mice) CD11c^{+} cells evaluated by FACS. (B) Distribution of CD11c^{+} (brown) and CD3^{+} (blue) cells in RAG2$^{+/+}$ and *RAG2*^{R229Q} spleens evaluated by immunohistochemistry (original magnification, ×10). (C) FACS evaluation of number (left; $^{**}P$=0.009; $^{***}P$=0.0008) and frequency distribution (right; $^{**}P$=0.0013; $^{**}P$=0.007) of splenic RAG2$^{+/+}$ and *RAG2*^{R229Q} cDCs, pDCs, and Mo-DCs (one representative experiment out of four; average of eight RAG2$^{+/+}$ and seven *RAG2*^{R229Q} mice). (D) Mean fluorescence intensity of MHCII expressed by DCs evaluated by FACS in untreated (UNT) mice (CD8^{+}cDCs, $^{*}P$=0.02; CD8^{-}cDCs, $^{*}P$=0.03) and 6 h after LPS treatment (CD8^{+}cDCs, $^{*}P$=0.01; CD8^{-}cDCs, $^{**}P$=0.0069; LPS, 100 ng/g mouse weight, i.p.). (E) FACS evaluation of splenic CD11c^{+} cell number before (t=0) and after (t=24, 48, and 72 h) in vivo LPS injection (1 μg/g mouse weight, i.p.).

subsets, with the exception of CD8^{+} cDCs. Moreover, defective migration of DCs to LNs in inflammatory conditions was demonstrated by skin painting and the CHS model, in which a reduced number of cutaneous DCs, in particular Langerin^{+} cells, were found in skin draining LNs. Interestingly, defective LC migration from skin to LNs and accumulation of LCs in the skin have been found in autoimmune diseases with cutaneous manifestations, such as lupus and psoriasis [28, 37]. We speculate that LCs, dislocated into the derma of mutant mice, may activate skin-infiltrating autoreactive T cells continuously [6, 28], thus perpetuating chronic skin inflammation. Furthermore, the reduced number of activated DCs found in draining LNs after cutaneous stimulation might concur to the reduced migration, although the correlation between DC maturation and its consequent migration is still controversial [44]. Although chemokines and cytokines have a crucial role in DC development, migration, and function, we did not detect relevant alterations sustaining the defects observed in our mutant mice. However, we cannot exclude that in in vivo inflammatory conditions, altered production of cytokines and chemokines may play a role in the impaired DC recruitment [45]. Furthermore, the altered OS LN architecture could influence DC retention, as demonstrated in other immunodeficient mice [12]. This hypothesis is supported by the lack of increase in LN cellularity in mutant mice upon CFSE-labeled BM-DC injection and the reduced number of CFSE^{+} RAG2$^{+/+}$ BM-DCs migrated into mutant LNs. Previous data have indicated the involvement of T cells in DC maturation [46] and demonstrated DC alterations in mouse models with defective T cell generation, such as athymic *nu/nu* mice [47], *ikaros*$^{-/-}$, and SCID mice [11]. Here, we showed that thymic DCs in *RAG2*^{R229Q} mice are reduced in number and express a lower level of the MHCII surface marker compared with RAG2$^{+/+}$ mice. These data well recapitulate the human phenotype in which a reduced amount of CD11c^{+} cells and absence of CD208 (DC-LAMP^{+}), a marker of activated DCs, have been reported [5, 13]. As thymic DC subsets are involved in negative selection and mediate nTreg cell induction [41], we hypoth-

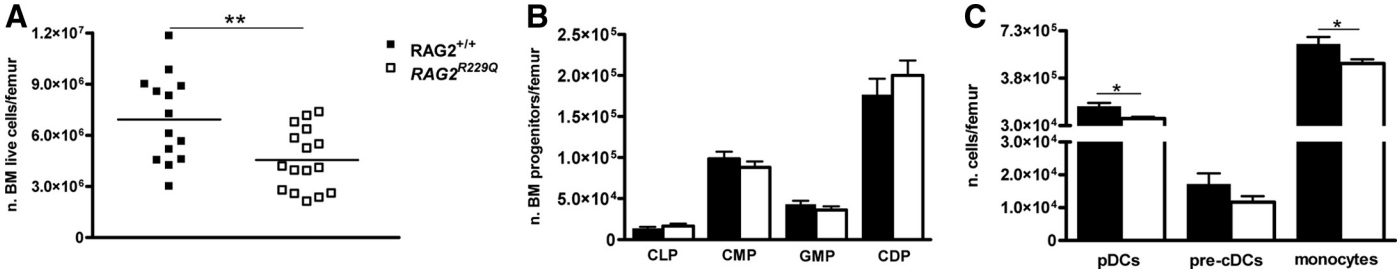

Figure 7. Reduction in pDC precursors and monocytes and normal number of DC progenitors and pre-cDCs in *RAG2*^{R229Q} BM. (A) BM cellularity was evaluated by FACS; the data are representative of RAG2$^{+/+}$ (average of 14 mice) and *RAG2*^{R229Q} BM samples (average of 16 mice) (**P=0.0058). (B) BM progenitors (CLP, CMP, GMP, and CDP) were evaluated by FACS [21–23] (see Materials and Methods for gating strategy) in BM samples, respectively, for each group of eight mice (one representative experiment out of two). (C) Number of pDCs, pre-cDCs, and monocytes in RAG2$^{+/+}$ and *RAG2*^{R229Q} BM samples (pDCs, *P=0.019; monocytes, *P=0.0259; two experiments performed; four mice/group).

esize that alterations in DC distribution and activation, together with mTEC deficiency and abnormal thymic structure [5, 6], could contribute to the defective central tolerance in OS. In addition, the high density of F4/80$^+$ macrophages in murine and patient thymus [13] might reflect, besides a role in clearance of apoptotic thymocytes [48, 49], an attempt of macrophages to act as APCs in the presence of few mTECs and DCs. The analysis of DC distribution in the spleen has also revealed a marked reduction in CD8$^+$ cDCs and pDCs, whereas CD8$^-$ cDCs, including Mo-DCs [19], were normally represented in number and increased in percentage. MHCII expression level in both cDC subsets was reduced at steady state and upon LPS-induced inflammatory conditions [29]. Interestingly, in vivo injection of high doses of LPS to induce DC apoptosis [30] showed no variation in the absolute counts of splenic *RAG2*^{R229Q} DCs. As the DC number is crucial for the maintenance of immune homeostasis, we can speculate that the persistence of *RAG2*^{R229Q} DCs might contribute to T cell activation, thus favoring increased susceptibility to autoimmunity [50, 51]. Furthermore, reduced DC number and activation state could also affect nTreg cell homeostasis and function [10]. Indeed, *RAG*^{R229Q} mice and OS patients showed a severe reduction in thymic and peripheral nTreg cells and impaired suppressive functions (refs. [3, 5, 8], and data not shown). When we evaluated whether the reduced DC counts would be caused by a defective number of their BM precursors [42], we detected a normal number of pre-cDCs and a reduction in pDC and monocyte absolute counts. Interestingly, up-regulation of MHCII upon LPS induction in BM-DCs was impaired, and BM-derived pDCs expressed a lower level of MHCII even at the steady-state condition. Of note, RAG genes are expressed in pDCs [52–54]; thus, it is likely that hypomorphic mutations in RAG genes could also impair the generation and function of pDCs. Overall, our data provide, for the first time, evidences of the effect of hypomorphic mutation in RAG genes on DC distribution and function, thus adding an additional layer of dysregulation to the mechanisms controlling central and peripheral tolerance.

AUTHORSHIP

V. Maina designed and performed research, analyzed data, and wrote the manuscript. P.L.P., E.F., and S.M. performed histological analyses. V. Marrella, B.C., A.A., and A.D.P. contributed to performing the experiments. P.V., P.L.P., and S.S. contributed to the revision of the manuscript. A.V. designed the research, analyzed the data, and wrote the manuscript.

ACKNOWLEDGMENTS

This work was supported by grants from the Fondazione Telethon and from the Fondazione Cariplo 2012-0519 (both to A.V.). This work was also supported by the European Commission's Seventh Framework Programme: 261387-Advanced Cell-Based Therapies for the Treatment of Primary ImmunoDeficiency (CELL-PID).

DISCLOSURES

The authors declare no financial interests.

REFERENCES

1. Villa, A., Notarangelo, L. D., Roifman, C. M. (2008) Omenn syndrome: inflammation in leaky severe combined immunodeficiency. *J. Allergy Clin. Immunol.* **122,** 1082–1086.
2. Marrella, V., Maina, V., Villa, A. (2011) Omenn syndrome does not live by V(D)J recombination alone. *Curr. Opin. Allergy Clin. Immunol.* **11,** 525–531.
3. Cassani, B., Poliani, P. L., Marrella, V., Schena, F., Sauer, A. V., Ravanini, M., Strina, D., Busse, C. E., Regenass, S., Wardemann, H., Martini, A., Facchetti, F., van der Burg, M., Rolink, A. G., Vezzoni, P., Grassi, F., Traggiai, E., Villa, A. (2010) Homeostatic expansion of autoreactive immunoglobulin-secreting cells in the Rag2 mouse model of Omenn syndrome. *J. Exp. Med.* **207,** 1525–1540.
4. Walter, J. E., Rucci, F., Patrizi, L., Recher, M., Regenass, S., Paganini, T., Keszei, M., Pessach, I., Lang, P. A., Poliani, P. L., Giliani, S., Al-Herz, W., Cowan, M. J., Puck, J. M., Bleesing, J., Niehues, T., Schuetz, C., Malech, H., DeRavin, S. S., Facchetti, F., Gennery, A. R., Andersson, E., Kamani, N. R., Sekiguchi, J., Alenezi, H. M., Chinen, J., Dbaibo, G., ElGhazali, G., Fontana, A., Pasic, S., Detre, C., Terhorst, C., Alt, F. W., Notarangelo, L. D. (2010) Expansion of immunoglobulin-secreting cells and defects in B cell tolerance in Rag-dependent immunodeficiency. *J. Exp. Med.* **207,** 1541–1554.
5. Marrella, V., Poliani, P. L., Casati, A., Rucci, F., Frascoli, L., Gougeon, M. L., Lemercier, B., Bosticardo, M., Ravanini, M., Battaglia, M., Roncarolo, M. G., Cavazzana-Calvo, M., Facchetti, F., Notarangelo, L. D., Vezzoni, P., Grassi, F., Villa, A. (2007) A hypomorphic R229Q Rag2 mouse mutant recapitulates human Omenn syndrome. *J. Clin. Invest.* **117,** 1260–1269.
6. Marrella, V., Poliani, P. L., Fontana, E., Casati, A., Maina, V., Cassani, B., Ficara, F., Cominelli, M., Schena, F., Paulis, M., Traggiai, E., Vezzoni, P., Grassi, F., Villa, A. (2012) Anti-CD3epsilon mAb improves thymic architecture and prevents autoimmune manifestations in a mouse model of Omenn syndrome: therapeutic implications. *Blood* **120,** 1005–1014.
7. Cavadini, P., Vermi, W., Facchetti, F., Fontana, S., Nagafuchi, S., Mazzolari, E., Sediva, A., Marrella, V., Villa, A., Fischer, A., Notarangelo, L. D., Badolato, R. (2005) AIRE deficiency in thymus of 2 patients with Omenn syndrome. *J. Clin. Invest.* **115,** 728–732.
8. Cassani, B., Poliani, P. L., Moratto, D., Sobacchi, C., Marrella, V., Imperatori, L., Vairo, D., Plebani, A., Giliani, S., Vezzoni, P., Facchetti, F., Porta, F.,

Notarangelo, L. D., Villa, A., Badolato, R. (2010) Defect of regulatory T cells in patients with Omenn syndrome. *J. Allergy Clin. Immunol.* **125,** 209–216.
9. Guermonprez, P., Valladeau, J., Zitvogel, L., Thery, C., Amigorena, S. (2002) Antigen presentation and T cell stimulation by dendritic cells. *Ann. Rev. Immun.* **20,** 621–667.
10. Darrasse-Jeze, G., Deroubaix, S., Mouquet, H., Victora, G. D., Eisenreich, T., Yao, K. H., Masilamani, R. F., Dustin, M. L., Rudensky, A., Liu, K., Nussenzweig, M. C. (2009) Feedback control of regulatory T cell homeostasis by dendritic cells in vivo. *J. Exp. Med.* **206,** 1853–1862.
11. Shreedhar, V., Moodycliffe, A. M., Ullrich, S. E., Bucana, C., Kripke, M. L., Flores-Romo, L. (1999) Dendritic cells require T cells for functional maturation in vivo. *Immunity* **11,** 625–636.
12. Asli, B., Lantz, O., DiSanto, J. P., Saeland, S., Geissmann, F. (2004) Roles of lymphoid cells in the differentiation of Langerhans dendritic cells in mice. *Immunobiology* **209,** 209–221.
13. Poliani, P. L., Facchetti, F., Ravanini, M., Gennery, A. R., Villa, A., Roifman, C. M., Notarangelo, L. D. (2009) Early defects in human T-cell development severely affect distribution and maturation of thymic stromal cells: possible implications for the pathophysiology of Omenn syndrome. *Blood* **114,** 105–108.
14. Emile, J. F., Durandy, A., Le Deist, F., Fischer, A., Brousse, N. (1997) Epidermal Langerhans' cells in children with primary T-cell immune deficiencies. *J. Pathol.* **183,** 70–74.
15. Facchetti, F., Blanzuoli, L., Ungari, M., Alebardi, O., Vermi, W. (1998) Lymph node pathology in primary combined immunodeficiency diseases. *Springer Semin. Immunopathol.* **19,** 459–478.
16. Villa, A., Santagata, S., Bozzi, F., Giliani, S., Frattini, A., Imberti, L., Gatta, L. B., Ochs, H. D., Schwarz, K., Notarangelo, L. D., Vezzoni, P., Spanopoulou, E. (1998) Partial V(D)J recombination activity leads to Omenn syndrome. *Cell* **93,** 885–896.
17. Signorini, S., Imberti, L., Pirovano, S., Villa, A., Facchetti, F., Ungari, M., Bozzi, F., Albertini, A., Ugazio, A. G., Vezzoni, P., Notarangelo, L. D. (1999) Intrathymic restriction and peripheral expansion of the T-cell repertoire in Omenn syndrome. *Blood* **94,** 3468–3478.
18. Cheong, C., Idoyaga, J., Do, Y., Pack, M., Park, S. H., Lee, H., Kang, Y. S., Choi, J. H., Kim, J. Y., Bonito, A., Inaba, K., Yamazaki, S., Steinman, R. M., Park, C. G. (2007) Production of monoclonal antibodies that recognize the extracellular domain of mouse langerin/CD207. *J. Immunol. Methods* **324,** 48–62.
19. Nakano, H., Lin, K. L., Yanagita, M., Charbonneau, C., Cook, D. N., Kakiuchi, T., Gunn, M. D. (2009) Blood-derived inflammatory dendritic cells in lymph nodes stimulate acute T helper type 1 immune responses. *Nat. Immunol.* **10,** 394–402.
20. Geissmann, F., Auffray, C., Palframan, R., Wirrig, C., Ciocca, A., Campisi, L., Narni-Mancinelli, E., Lauvau, G. (2008) Blood monocytes: distinct subsets, how they relate to dendritic cells, and their possible roles in the regulation of T-cell responses. *Immunol. Cell Biol.* **86,** 398–408.
21. Bursch, L. S., Wang, L., Igyarto, B., Kissenpfennig, A., Malissen, B., Kaplan, D. H., Hogquist, K. A. (2007) Identification of a novel population of Langerin+ dendritic cells. *J. Exp. Med.* **204,** 3147–3156.
22. Merad, M., Ginhoux, F., Collin, M. (2008) Origin, homeostasis and function of Langerhans cells and other Langerin-expressing dendritic cells. *Nat. Rev. Immunol.* **8,** 935–947.
23. Schmid, M. A., Kingston, D., Boddupalli, S., Manz, M. G. (2010) Instructive cytokine signals in dendritic cell lineage commitment. *Immunol. Rev.* **234,** 32–44.
24. Schmid, M. A., Takizawa, H., Baumjohann, D. R., Saito, Y., Manz, M. G. (2011) Bone marrow dendritic cell progenitors sense pathogens via Toll-like receptors and subsequently migrate to inflamed lymph nodes. *Blood* **118,** 4829–4840.
25. Kondo, M., Wagers, A. J., Manz, M. G., Prohaska, S. S., Scherer, D. C., Beilhack, G. F., Shizuru, J. A., Weissman, I. L. (2003) Biology of hematopoietic stem cells and progenitors: implications for clinical application. *Ann. Rev. Immunol.* **21,** 759–806.
26. Roederer, M. (2002) Compensation in flow cytometry. *Curr. Protoc. Cytom.* Chapter 1, Unit 1.14.
27. Del Prete, A., Vermi, W., Dander, E., Otero, K., Barberis, L., Luini, W., Bernasconi, S., Sironi, M., Santoro, A., Garlanda, C., Facchetti, F., Wymann, M. P., Vecchi, A., Hirsch, E., Mantovani, A., Sozzani, S. (2004) Defective dendritic cell migration and activation of adaptive immunity in PI3Kγ-deficient mice. *EMBO J.* **23,** 3505–3515.
28. Eriksson, A. U., Singh, R. R. (2008) Cutting edge: migration of Langerhans dendritic cells is impaired in autoimmune dermatitis. *J. Immunol.* **181,** 7468–7472.
29. Kobayashi, T., Walsh, P. T., Walsh, M. C., Speirs, K. M., Chiffoleau, E., King, C. G., Hancock, W. W., Caamano, J. H., Hunter, C. A., Scott, P., Turka, L. A., Choi, Y. (2003) TRAF6 is a critical factor for dendritic cell maturation and development. *Immunity* **19,** 353–363.
30. Zanoni, I., Ostuni, R., Capuano, G., Collini, M., Caccia, M., Ronchi, A. E., Rocchetti, M., Mingozzi, F., Foti, M., Chirico, G., Costa, B., Zaza, A., Ricciardi-Castagnoli, P., Granucci, F. (2009) CD14 regulates the dendritic cell life cycle after LPS exposure through NFAT activation. *Nature* **460,** 264–268.
31. Merad, M., Hoffmann, P., Ranheim, E., Slaymaker, S., Manz, M. G., Lira, S. A., Charo, I., Cook, D. N., Weissman, I. L., Strober, S., Engleman, E. G. (2004) Depletion of host Langerhans cells before transplantation of donor alloreactive T cells prevents skin graft-versus-host disease. *Nat. Med.* **10,** 510–517.
32. Mayerova, D., Parke, E. A., Bursch, L. S., Odumade, O. A., Hogquist, K. A. (2004) Langerhans cells activate naive self-antigen-specific CD8 T cells in the steady state. *Immunity* **21,** 391–400.
33. Shinzato, M., Shamoto, M., Hosokawa, S., Kaneko, C., Osada, A., Shimizu, M., Yoshida, A. (1995) Differentiation of Langerhans cells from interdigitating cells using CD1a and S-100 protein antibodies. *Biotech. Histochem.* **70,** 114–118.
34. Rezk, S. A., Agrawal, R., Weiss, L. M. (2012) Do indeterminate cells follow the footsteps of Langerhans cells and migrate from the skin to the lymph node? *Appl. Immunohistochem. Mol. Morphol.* **20,** 56–61.
35. Ratzinger, G., Burgdorf, W. H., Metze, D., Zelger, B. G., Zelger, B. (2005) Indeterminate cell histiocytosis: fact or fiction? *J. Cutan. Pathol.* **32,** 552–560.
36. Honda, T., Egawa, G., Grabbe, S., Kabashima, K. (2013) Update of immune events in the murine contact hypersensitivity model: toward the understanding of allergic contact dermatitis. *J. Invest. Dermatol.* **133,** 303–315.
37. Cumberbatch, M., Singh, M., Dearman, R. J., Young, H. S., Kimber, I., Griffiths, C. E. (2006) Impaired Langerhans cell migration in psoriasis. *J. Exp. Med.* **203,** 953–960.
38. MartIn-Fontecha, A., Sebastiani, S., Hopken, U. E., Uguccioni, M., Lipp, M., Lanzavecchia, A., Sallusto, F. (2003) Regulation of dendritic cell migration to the draining lymph node: impact on T lymphocyte traffic and priming. *J. Exp. Med.* **198,** 615–621.
39. Webster, B., Ekland, E. H., Agle, L. M., Chyou, S., Ruggieri, R., Lu, T. T. (2006) Regulation of lymph node vascular growth by dendritic cells. *J. Exp. Med.* **203,** 1903–1913.
40. Stutte, S., Quast, T., Gerbitzki, N., Savinko, T., Novak, N., Reifenberger, J., Homey, B., Kolanus, W., Alenius, H., Forster, I. (2010) Requirement of CCL17 for CCR7- and CXCR4-dependent migration of cutaneous dendritic cells. *Proc. Natl. Acad. Sci. USA* **107,** 8736–8741.
41. Proietto, A. I., van Dommelen, S., Wu, L. (2009) The impact of circulating dendritic cells on the development and differentiation of thymocytes. *Immunol. Cell. Biol.* **87,** 39–45.
42. Geissmann, F., Manz, M. G., Jung, S., Sieweke, M. H., Merad, M., Ley, K. (2010) Development of monocytes, macrophages, and dendritic cells. *Science* **327,** 656–661.
43. Waithman, J., Allan, R. S., Kosaka, H., Azukizawa, H., Shortman, K., Lutz, M. B., Heath, W. R., Carbone, F. R., Belz, G. T. (2007) Skin-derived dendritic cells can mediate deletional tolerance of class I-restricted self-reactive T cells. *J. Immunol.* **179,** 4535–4541.
44. Geissmann, F., Dieu-Nosjean, M. C., Dezutter, C., Valladeau, J., Kayal, S., Leborgne, M., Brousse, N., Saeland, S., Davoust, J. (2002) Accumulation of immature Langerhans cells in human lymph nodes draining chronically inflamed skin. *J. Exp. Med.* **196,** 417–430.
45. Mantovani, A., Bonecchi, R., Locati, M. (2006) Tuning inflammation and immunity by chemokine sequestration: decoys and more. *Nat. Rev. Immunol.* **6,** 907–918.
46. Kitajima, T., Caceres-Dittmar, G., Tapia, F. J., Jester, J., Bergstresser, P. R., Takashima, A. (1996) T cell-mediated terminal maturation of dendritic cells: loss of adhesive and phagocytotic capacities. *J. Immunol.* **157,** 2340–2347.
47. Grabbe, S., Gallo, R. L., Lindgren, A., Granstein, R. D. (1993) Deficient antigen presentation by Langerhans cells from athymic (nu/nu) mice. Restoration with thymic transplantation or administration of cytokines. *J. Immunol.* **151,** 3430–3439.
48. Szondy, Z., Garabuczi, E., Toth, K., Kiss, B., Koroskenyi, K. (2012) Thymocyte death by neglect: contribution of engulfing macrophages. *Eur. J. Immunol.* **42,** 1662–1667.
49. Surh, C. D., Sprent, J. (1994) T-cell apoptosis detected in situ during positive and negative selection in the thymus. *Nature* **372,** 100–103.
50. Chen, M., Wang, Y. H., Wang, Y., Huang, L., Sandoval, H., Liu, Y. J., Wang, J. (2006) Dendritic cell apoptosis in the maintenance of immune tolerance. *Science* **311,** 1160–1164.
51. Yamazaki, S., Iyoda, T., Tarbell, K., Olson, K., Velinzon, K., Inaba, K., Steinman, R. M. (2003) Direct expansion of functional CD25+ CD4+ regulatory T cells by antigen-processing dendritic cells. *J. Exp. Med.* **198,** 235–247.
52. Sathe, P., Vremec, D., Wu, L., Corcoran, L., Shortman, K. (2013) Convergent differentiation: myeloid and lymphoid pathways to murine plasmacytoid dendritic cells. *Blood* **121,** 11–19.
53. Luo, X. M., Lei, M. Y. (2012) Recombination activating gene-2 regulates CpG-mediated interferon-α production in mouse bone marrow-derived plasmacytoid dendritic cells. *PloS One* **7,** e47952.
54. Shigematsu, H., Reizis, B., Iwasaki, H., Mizuno, S., Hu, D., Traver, D., Leder, P., Sakaguchi, N., Akashi, K. (2004) Plasmacytoid dendritic cells activate lymphoid-specific genetic programs irrespective of their cellular origin. *Immunity* **21,** 43–53.

KEY WORDS:
Omenn syndrome · primary immunodeficiency · immune dysregulation